ChemComm

Accepted Manuscript

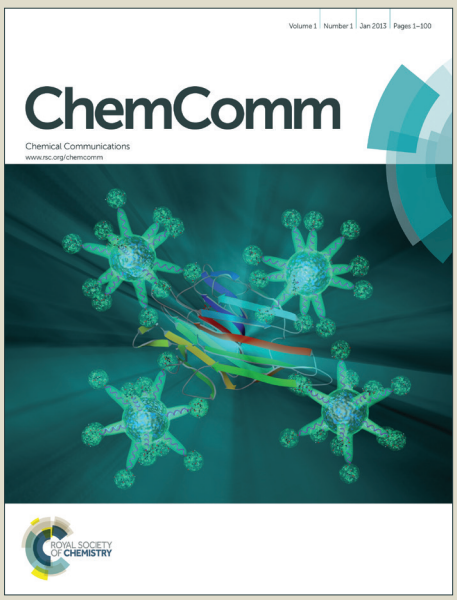

ROYAL SOCIETY OF CHEMISTRY

www.rsc.org/chemcomm

Journal Name

RSCPublishing

COMMUNICATION

Chemically–induced redox switching of a metalloprotein reveals thermodynamic and kinetic heterogeneity, one molecule at a time†

Cite this: DOI: 10.1039/x0xx00000x

Received ooth January 2012,
Accepted ooth January 2012

DOI: 10.1039/x0xx00000x

www.rsc.org/

Namik Akkilic*, Fenna van der Grient, Muhammad Kamran, Nusrat J.M. Sanghamitra

Oxidation (off state) and reduction (on state) of a single azurin molecule is monitored, one electron at a time, which depend on the chemical redox potential. By analysing of the fluorescence time traces from individual azurin molecules, reaction kinetics and redox thermodynamics were determined.

An overwhelming number of chemical reactions in nature, both in the living cell and in the inanimate world are redox reactions. When two compounds engage in such a reaction, one will be reduced, the other oxidized. The study of biological electron transfer (ET) reactions of proteins is not only crucial for our knowledge of many physiological functions such as cellular respiration, photosynthesis, and redox homeostasis,[1,2] but also for potential applications in biotechnology which drives the current proliferation of research on biofuel cells, protein biochips and biosensors.[3] The ability to monitor redox reactions of proteins and enzymes with high sensitivity is scientifically and commercially of great importance. However, the ensemble techniques such as conventional (spectro)electrochemistry are not sufficient and sensitive to determine redox parameters one molecule at a time.[4]

Instead of monitoring the concentration change of the substrate or the product to measure the reaction rate, a single–molecule (SM) experiment follows individual catalytic turnovers in real time and records the waiting times (τ) for completing individual reactions.[5] SM kinetic theories have been developed to explore underlying reaction mechanisms and the associated kinetic models by analysing probability distributions and statistical properties of the waiting time parameters.[6]

Recently, a Förster resonance energy transfer (FRET)–based method, so–called FluRedox principle, was developed to monitor the redox state of fluorescently labelled azurin molecules (Fig. S1, ESI†).[7,8] Azurin acts as an electron shuttle in ET chains and displays a strong absorption band at ~600 nm in the oxidized (Cu^{2+}) state, which is absent in the reduced (Cu^{+}) state (Fig. S2, ESI†).[7,9] Thus it is inferred that FRET from the fluorescent label (donor) to the Cu center (acceptor) occurs in the oxidized, but not in the reduced state of azurin.[7,8,10,11] Notably, FRET–based detection is highly selective with unmatched sensitivity, features that are very promising for biosensor applications.[12–15] Most importantly, the enhanced sensitivity has been applied for the SM detection of redox turn–over of several proteins and enzymes on glass substrates.[11,15–20] Moreover, it was shown that the FRET principle can be combined with electrochemistry, by which kinetic and thermodynamic heterogeneity of azurin[10,15,21,22] and nitrite turnover rate of a nitrite reductase[23] on gold electrodes were investigated.

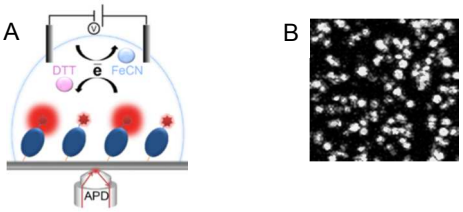

Fig. 1. A) Single molecule fluorescence detection of azurin–Cy5 molecules. The redox state of the protein was monitored using a mixture of DTT and $K_3(FeCN)_6$ as reductant and oxidant in the buffer solution. The redox potential of the solution was determined with a reference electrode (SCE) and counter electrode (Pt wire) connected to a voltmeter. B) The confocal image (10x10 μm^2) of Az–Cy5 immobilized on a glass surface with a dwell time of 2 ms per pixel.

Herein, we report direct monitoring of ET of fluorescently labeled wild–type azurin (wt–Az) molecules on a "passive" surface which reveals the midpoint potential (E_0) and reaction kinetics (k_{red} and k_{ox}) at the SM level. The protein was covalently immobilized on triethoxysilane (TES)–mercaptopropyl trimethoxysilane (MPTS) modified glass surface (Fig. 1A). To obtain a monodisperse and homogenous sample[15,24] for the SM experiments, Az was purified using high resolution anion exchange chromatography after labeling with Cy5–NHS (Fig. S3, ESI†).[15] The use of such a homogeneous sample is essential for consistent recordings of the fluorescence dynamics of SMs of labeled azurin. In order to ascertain the redox–

based fluorescence switching of the individual azurin molecules immobilized on a MPTS/TES coated glass substrate, we tuned the chemical redox potential (E) of the solution around the midpoint potential (E_0) of Az by means of varying the concentration of oxidant and/or reductant (Fig. 1A). The final redox potentials of the solution (E) were adjusted to –20, 0, 20, 40, 60, 80 and 100 mV, respectively, as measured with a reference electrode (standard calomel, SCE) and a counter electrode (Pt wire) which were inserted in the droplet that covered the functionalized glass substrate. The two electrodes were wired to a voltmeter.

At each potential, fluorescence time traces (Fig. S4) were obtained by successively parking the laser for excitation at each Az–Cy5 molecule in the confocal image (Fig. 1B), and then recording the arrival times of the emitted photons. Time traces were obtained for durations of up to 1 minute. Photobleaching of Cy5 limited the time duration for which photon emission could be observed to tens of seconds, and was marked by a drop of the count rate to background levels in a single step. The sample was de-aerated beforehand by bubbling with argon, and the measurements were performed under oxygen–free conditions in a sealed cell. This approach is not only improved the stability of the redox potential, but also enhanced the photostability of Az–Cy5, extending the time at which photobleaching occurred by at least an order of magnitude. Occasional blinking is attributed to the photophysical behavior of Cy5.[25] The events are relatively rare, and are not counted as a redox transition.

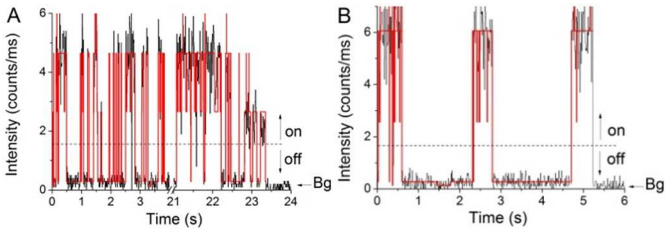

Fig. 2. The real time fluorescence intensity traces of a single azurin molecule with a 10 ms bin size (black) and calculated intensity change–point states (red) overlaid as a function of time. They exhibit an on–off switching behavior which depends on the redox potential in solution: A) E = 20 mV ($\overline{P}_{ox}$ = 0.52) B) E = 60 mV ($\overline{P}_{ox}$ = 0.76) vs. SCE.

Typical time traces are shown in Fig. 2 for two single–Az–Cy5 molecules. The time profiles show a pronounced fluorescence switching behaviour, and appear to be dominated by two discrete intensity levels, corresponding to the oxidized (off) and the reduced (on) state. To determine the intensity change points based on individual photon arrival times, a change point (CP) analysis[26] was applied to the experimental data which accurately reproduced (red lines, Fig. 2). The observed fluorescence time profile (black line) of Az–Cy5 depends on the redox potential in solution: It is estimated that the fraction of molecules that are actively switching is about 50% at 20 and 40 mV (~midpoint potential of Az), and is decreasing at higher and lower redox potentials, dropping to about 10% at –20 and 100 mV. At each potential, it is possible to calculate the parameter $\overline{P}_{ox}$ ($\overline{P}_{red}$), the time–averaged probability that the molecule is in the oxidized (reduced) state (Eq. 2, ESI†). For the particular two time traces in Fig. 2, $\overline{P}_{ox}$= 0.76 (mostly in the oxidized state) at a potential of 60 mV, while $\overline{P}_{ox}$ = 0.52 at 20 mV. No redox switching was observed at potentials higher than 100 mV and lower than –20 mV: the molecule is either fully oxidized or reduced, respectively. This assignment is supported by the fact that the control sample of Cy5–labeled Zn-Az and Cy5[10] did not show any fluorescence switching under the same conditions (Figs. S5 and S6, ESI†).

Fluorescence switching ratio (SR) (Eq. 16, ESI†) of individual Az–Cy5 molecules are calculated by using the intensity values in the reduced (I_{red}) and oxidized (I_{ox}) states, obtained from the CP analysis (Fig. 2). Because of the high SR, the fluorescence intensity of an oxidized Az–Cy5 molecule (off state) is rather close to the background level. The histogram in Fig. 3A shows the distribution of fluorescence SRs of individual azurin molecules immobilized on a glass surface. The average is 87 ±5%, in good agreement with that the SR of redox–induced fluorescence switching in bulk[15] (Fig. S6A, ESI†). Although the distribution of SM–Az SRs is narrow, it is possibly associated with, at least partially, (average) variations in distance of Cy5 to the redox center by virtue of the length of the linker. The higher SR values we obtained compared to the previous work ($SR = 77\%$)[8,10] can be attributed to the purification of azurin after labeling with the fluorophore.

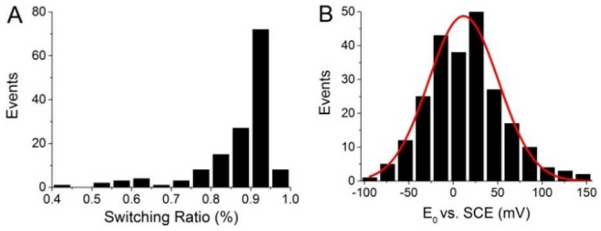

Fig. 3. A) FRET–based fluorescence switching ratio (SR) of individual Az–Cy5 molecules. The average SR of 87 ± 5% correlates well with that of Az–Cy5 in bulk solution (Fig. S6A, ESI†). B) The histogram of midpoint potential (E_0) of about 200 single azurin molecules. The average E_0 was calculated from a Gaussian fit (red curve) as 12 ±3 mV with a fwhm = 92 mV vs SCE. E_0 of each single molecule was calculated using the Nernst equation (Eq. 10, ESI†).

Furthermore, we calculated the midpoint potential (E_0) of each single Az–Cy5 molecule by replacing the concentration gradient ($[Az_{red}]/[Az_{ox}]$) in the Nernst equation to gradient of the time–averaged probability ($\overline{P}_{red}/\overline{P}_{ox}$) (Eq 10, ESI†). The result of such calculations is summarized in Fig. S7, which shows the distributions of the obtained midpoint potentials (E_0) for each of the chemically adjusted redox potentials. The E_0 values range from –100 to 150 mV which is consistent with electrochemical data.[15,21,27] We observe that the measured distribution of midpoint potentials shifts with the actual redox potential of the solution. This can be explained by the fact that the data contain a bias towards selection of Az–Cy5 molecules that are relatively bright. Because of the high SR, molecules that are mostly in the oxidized state are under–represented because of low visibility. The calculated midpoint potentials for 200 individual molecules are shown in the histogram (Fig. 3B). The average midpoint potential is 12 ±3 mV vs SCE, and the Gaussian distribution is characterized by a full width at half maximum (FWHM) of 92 mV.

This result is similar to that the values of E_0=6 ±0.6 mV vs SCE for the high–coverage (about 1000 molecules, FWHM=150 mV)[10] and E_0=16 mV vs SCE for the low–coverage (100–450 molecules, FWHM=70 mV) data on semi–transparent Au electrode.[21] Hence, the E_0 values we observed are consistent with the previously reported midpoint

potentials of 1–10 μM azurin in solution for the fluorescence (293 mV vs NHE) and for the absorption (291 mV vs NHE) titration.[8] However, distribution of midpoint potentials is significantly larger than the electrochemically obtained switching of Az–Cy5 on gold electrode both, at the SM level[15] and with high–density coverage[21] (FWHM=14–15 mV). This is due to the fact that, hydrophobic patch on the protein surface which is close to the azurin Cu center is believed to orient towards the hydrophobic alkanethiol head groups, leading to a favorable orientation for electron transfer.[27,28]

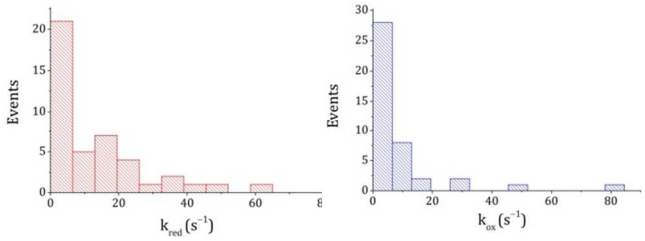

Fig. 4. The histogram of the reaction rates of individual Az–Cy5 molecules.

The ET rates for the oxidation (k_{off}) and reduction reaction (k_{on}) of a SM can be derived from the dwell time distributions i.e. the times the molecule stays in a certain state before jumping to the other state. The rate constants, k_{on} and k_{off} (Fig. S8), are calculated as 10 s^{-1} and 6 s^{-1} for a single Az–Cy5 molecule (Fig. 2, E = 20 mV) by the inverse of the characteristic time constants of the mono–exponential fits of the distributions, respectively. Fig. 4 shows the distribution of reaction rates of oxidized (off) and reduced (on) states of about 45 single Az–Cy5 molecules. The reaction rates for on and off states in Fig. 4 are relatively distributed homogeneous between ~1–20 s^{-1}.

Although, there are no data in the literature by which these values can be compared directly, our rate constants are similar to the ones that were measured for direct ET between the gold electrode and azurin adsorbed on 3,3'-dithiobis(sulfosuccinimidylpropionate) (2–6 s^{-1}),[29] mercaptosuccinic acid (3–6 s^{-1})[30] and hexanethiol (4–12 s^{-1})[31] self–assembled monolayers (SAMs). Besides, ET kinetics of azurin adsorbed on gold electrode depends on the distance of redox center to the electrode surface. Increasing the number of methylene units in the alkanethiols resulted in significant peak splitting and leads to slow ET rates.[32,33] At low surface coverages distribution of azurin molecules immobilized on gold electrode, also showed very low ET rate of 0.5–2 s^{-1} with a high-k tail up to 100 s^{-1}.[21] Moreover, intramolecular long range ET for azurin was shown to be pH dependent: at high pH the k value decreased from 285 to 15 s^{-1}.[34]

It is well established that the electrostatic environment of the entire protein and solvent system is a determining factor in fine–tuning the electronic properties of the metal–binding site of copper–containing proteins.[35,36] In particular, hybrid quantum mechanics/molecular mechanics model calculations show a significant solvent rearrangement in a region close to the copper ion, specifically, around the copper–bound His117 residue upon reduction.[37] It is claimed that the water rearrangement accounts for ~80% of the calculated value of the reorganization energy in this process. A similar conclusion was reached on the basis of experiments on electron tunneling in azurin crystals.[38] Presumably the rearrangement is driven by modification of the electrostatic potential at the protein surface around His117, reflecting the change in the oxidation state of Cu. It may also affect the conformation of solvent–exposed side chains. It thus seems reasonable to conclude that the local variations in the outer sphere around His117 can contribute to variations in the midpoint potential of individual azurin molecules.[35–37] This residue, which has a key role in the ET reaction of azurin, is normally in direct contact with the solvent. It may be assumed that under those conditions, Az–Cy5 behaves as a free molecule in solution with the His117 residue fully exposed to the solvent environment. This is different from azurin immobilized on conductive electrodes[10,15,21,27,28] where the hydrophobic patch of the protein around His117 is largely shielded from the solution. In fact, at the hydrophobic interface between the protein and the self–assembled monolayer, most water molecules will be expelled. The result is a more homogeneous and a more static environment of the His117 residue than for azurin in solution. This is reflected in the relatively small heterogeneity of the midpoint potential,[15,21] compared to that of Az–Cy5 in solution.

To conclude, we were able to make a quantitative assessment of the heterogeneity of the redox parameters, for the first time, for individual azurin molecules, covalently immobilized on a "passive" surface. The FRET–based, chemically–induced redox switching can be easily applied to e.g. cytochrome c551, nitrite reductase, and several dehydrogenases to study interprotein ET reactions at the SM sensitivity. Further work on this subject is under way.

We thank Prof. H. Yang for the changepoint analysis algorithm, Prof. T.J. Aartsma, Prof. G.W. Canters, Dr. A. Andreoni for the scientific discussions. This work was supported by the European Commission through the EdRox Network (contract no. MRTN–CT–2006–035649).

Notes and references

Biological and Soft Matter Physics, LION, Leiden University, Niels Bohrweg 2, 2333 CA Leiden, the Netherlands
E-mail: namikakkilic@gmail.com

† Electronic Supplementary Information (ESI) available: [Experimental procedures, data elaboration and analysis are included in the supporting information]. See DOI: 10.1039/c000000x/

1. G. F. Moore and G. W. Brudvig, *Annu. Rev. Condens. Matter Phys.*, 2011, **2**, 303–327.
2. B. E. Ramirez, B. G. Malmström, J. R. Winkler, and H. B. Gray, *Proc. Natl. Acad. Sci. U. S. A.*, 1995, **92**, 11949–51.
3. I. Willner, *Science*, 2002, **298**, 2407–8.
4. S. G. Lemay, S. Kang, K. Mathwig, and P. S. Singh, *Acc. Chem. Res.*, 2013, **46**, 369–77.
5. V. I. Claessen, H. Engelkamp, P. C. M. Christianen, J. C. Maan, R. J. M. Nolte, K. Blank, and A. E. Rowan, *Annu. Rev. Anal. Chem.*, 2010, **3**, 319–40.
6. B. P. English, W. Min, A. M. van Oijen, K. T. Lee, G. Luo, H. Sun, B. J. Cherayil, S. C. Kou, and X. S. Xie, *Nat. Chem. Biol.*, 2006, **2**, 87–94.
7. R. Schmauder, S. Alagaratnam, C. Chan, T. Schmidt, G. W. Canters, and T. J. Aartsma, *J. Biol. Inorg. Chem.*, 2005, **10**, 683–7.
8. S. Kuznetsova, G. Zauner, R. Schmauder, O. A. Mayboroda, A. M. Deelder, T. J. Aartsma, and G. W. Canters, *Anal. Biochem.*, 2006, **350**, 52–60.
9. E. Solomon and J. Hare, *J. Am. Chem. Soc.*, 1980, **102**, 168–178.

10. J. J. Davis, H. Burgess, G. Zauner, S. Kuznetsova, J. Salverda, T. Aartsma, and G. W. Canters, *J. Phys. Chem. B*, 2006, **110**, 20649–54.
11. R. Schmauder, F. Librizzi, G. W. Canters, T. Schmidt, and T. J. Aartsma, *Chemphyschem*, 2005, **6**, 1381–6.
12. G. Zauner, E. Lonardi, L. Bubacco, T. J. Aartsma, G. W. Canters, and A. W. J. W. Tepper, *Chem. Eur. J.*, 2007, **13**, 7085–90.
13. M. Strianese, G. Zauner, A. W. J. W. Tepper, L. Bubacco, E. Breukink, T. J. Aartsma, G. W. Canters, and L. C. Tabares, *Anal. Biochem.*, 2009, **385**, 242–8.
14. M. Gustiananda, A. Andreoni, L. C. Tabares, A. W. J. W. J. W. Tepper, L. Fortunato, T. J. Aartsma, and G. W. Canters, *Biosens. Bioelectron.*, 2011, **31**, 419–25.
15. N. Akkilic, M. Kamran, R. Stan, and N. J. M. Sanghamitra, *Biosens. Bioelectron.*, 2014. DOI: 10.1016/j.bios.2014.07.051.
16. S. Kuznetsova, G. Zauner, T. J. Aartsma, H. Engelkamp, N. Hatzakis, A. E. Rowan, R. J. M. Nolte, P. C. M. Christianen, and G. W. Canters, *Proc. Natl. Acad. Sci. U. S. A.*, 2008, **105**, 3250–5.
17. L. C. Tabares, D. Kostrz, A. Elmalk, A. Andreoni, C. Dennison, T. J. Aartsma, and G. W. Canters, *Chem. A Eur. J.*, 2011, **17**, 12015–9.
18. A. T. Elmalk, J. M. Salverda, L. C. Tabares, G. W. Canters, and T. J. Aartsma, *J. Chem. Phys.*, 2012, **136**, 235101.
19. R. H. Goldsmith, L. C. Tabares, D. Kostrz, C. Dennison, T. J. Aartsma, G. W. Canters, and W. E. Moerner, *Proc. Natl. Acad. Sci. U. S. A.*, 2011, **108**, 17269–74.
20. A. Gupta, T. J. Aartsma, and G. W. Canters, *J. Am. Chem. Soc.*, 2014, **136**, 2707–10.
21. J. M. Salverda, A. V. Patil, G. Mizzon, S. Kuznetsova, G. Zauner, N. Akkilic, G. W. Canters, J. J. Davis, H. A. Heering, and T. J. Aartsma, *Angew. Chemie Int. Ed.*, 2010, **49**, 5776–9.
22. A. V. Patil and J. J. Davis, *J. Am. Chem. Soc.*, 2010, **132**, 16938–44.
23. Ł. Krzemiński, L. Ndamba, G. W. Canters, T. J. Aartsma, S. D. Evans, and L. J. C. Jeuken, *J. Am. Chem. Soc.*, 2011, **133**, 15085–93.
24. S. Nicolardi, A. Andreoni, L. C. Tabares, Y. E. M. van der Burgt, G. W. Canters, A. M. Deelder, and P. J. Hensbergen, *Anal. Chem.*, 2012, **84**, 2512–20.
25. T. Ha and P. Tinnefeld, *Annu. Rev. Phys. Chem.*, 2012, **63**, 595–617.
26. L. P. Watkins and H. Yang, *J. Phys. Chem. B*, 2005, **109**, 617–28.
27. L. J. C. Jeuken and F. A. Armstrong, *J. Phys. Chem. B*, 2001, **105**, 5271–5282.
28. Q. Chi, O. Farver, and J. Ulstrup, *Proc. Natl. Acad. Sci. U. S. A.*, 2005, **102**, 16203–16208.
29. S. Shleev, J. Wetterö, K.-E. Magnusson, and T. Ruzgas, *Biosens. Bioelectron.*, 2006, **22**, 213–9.
30. F. Lisdat and I. Karube, *Biosens. Bioelectron.*, 2002, **17**, 1051–7.
31. A. Gaigalas and G. Niaura, *J. Colloid Interface Sci.*, 1997, **193**, 60–70.
32. M. L. Vargo, C. P. Gulka, J. K. Gerig, C. M. Manieri, J. D. Dattelbaum, C. B. Marks, N. T. Lawrence, M. L. Trawick, and M. C. Leopold, *Langmuir*, 2010, **26**, 560–9.
33. D. E. Khoshtariya, T. D. Dolidze, M. Shushanyan, K. L. Davis, D. H. Waldeck, and R. van Eldik, *Proc. Natl. Acad. Sci. U. S. A.*, 2010, **107**, 2757–62.
34. O. Farver, N. Bonander, L. Skov, and I. Pecht, *Inorganica Chim. Acta*, 1996, **243**, 127–133.
35. J. Liu, S. Chakraborty, P. Hosseinzadeh, Y. Yu, S. Tian, I. Petrik, A. Bhagi, and Y. Lu, *Chem. Rev.*, 2014, **114**, 4366–469.
36. J. R. Winkler and H. B. Gray, *Chem. Rev.*, 2014, **114**, 3369–80.
37. M. Cascella, A. Magistrato, I. Tavernelli, P. Carloni, and U. Rothlisberger, *Proc. Natl. Acad. Sci. U. S. A.*, 2006, **103**, 19641–6.
38. B. R. Crane, A. J. Di Bilio, J. R. Winkler, and H. B. Gray, *J. Am. Chem. Soc.*, 2001, **123**, 11623–11631.